Hindawi
International Journal of Aerospace Engineering
Volume 2024, Article ID 8703004, 20 pages
https://doi.org/10.1155/2024/8703004

Research Article

Design, Multiperspective Investigations, and Performance Analysis of Multirotor Unmanned Aerial Vehicle for Precision Farming

Darshan Kumar Jayaram,[1] **Vijayanandh Raja**,[1] **Beena Stanislaus Arputharaj**,[2] **and Hussein A. Z. AL-bonsrulah**[3,4]

[1]*Department of Aeronautical Engineering, Kumaraguru College of Technology, Coimbatore, Tamil Nadu, India*
[2]*Department of Research and Innovation, Saveetha School of Engineering, SIMATS, Chennai 602105, Tamil Nadu, India*
[3]*Mechanical Power Technical Engineering Department, Al-Amarah University College, Maysan, Iraq*
[4]*Department of Computer Techniques Engineering, AlSafwa University College, Karbala, Iraq*

Correspondence should be addressed to Darshan Kumar Jayaram; darshankumar.j.aeu@kct.ac.in and Vijayanandh Raja; vijayanandh.raja@gmail.com

Received 5 February 2023; Revised 26 November 2023; Accepted 11 January 2024; Published 23 February 2024

Academic Editor: Jacopo Serafini

Farming and agriculture are the oldest professions, but they are adapting to the technology revolution to accommodate the world's growing population. UAV technology is part of the agriculture revolution, which aims to boost crop yields, properly monitor fields, and handle manpower shortages and resource efficiency. Rural India's tiny farmers cannot afford UAV technology; therefore, it has not yet spread. Payload capacity, endurance, and selective spraying are other considerations. Thus, a low-cost, long-lasting UAV is necessary. This study modified the arm assembly to create a cheap hexacopter UAV. The endurance increased by 10% when 1.5 kg was lost. ABS plastic was used to make the modular arm. For working loads of 9 kg and 10 kg, pesticide/fertilizer spraying saves time, money, and manpower. Thus, a pressure-area coverage-cone angle connection is needed. This study examined spray patterns at different pressures and heights by varying flat fan nozzle and complete cone nozzle orifice diameters. These factors were linked, helping farmers choose the right nozzle. This nozzle was installed in the UAV and field-tested for paddy crops, showing a significant production improvement and lower operational cost. Chemical use pollutes and leaves traces in produce. Precision farming with artificial intelligence (AI) has solved this problem. In this experiment, AI algorithms were used to lemon leaves. Three AI systems were tested on different datasets to forecast plant stress by analyzing leaves due to technical constraints. CNN's accuracy and computing speed make it ideal for precision farming. This work's UAV was 30% cheaper than commercial UAVs and had more durability. Farmers will also benefit from the flat fan and complete cone nozzles' pressure-area coverage connection.

1. Introduction

Industry and agriculture have been affected by automation and mechanisation. Monsoon failure and unseasonal rain due to global warming hurt crops [1]. India's 40% GDP comes from agriculture, with most farmers having less than a hectare of land and earning less than 300 Indian rupees a day [2, 3]. Agriculture workers are relocating to cities for better pay and job security [4].

Agriculture is expensive due to a lack of irrigation water, fertilizers, and labor. IoT, drip irrigation, UAV spraying, and crop health monitoring are used by even small farmers to solve these issues [5]. Compared to autonomous tractors and other pricey methods, UAV fertilizer spraying seems economical and user-friendly [6]. Thus, UAV use is rising exponentially, and the Indian government encourages it to double farmers' revenue. Therefore, it is necessary to build cost-effective, stable UAVs with better endurance, nozzles with wider coverage area, and leaf health monitoring utilizing an AI-based vision system for selecting crops. Thus, trends in agriculture, cost-effective UAV development, AI for leaf health prediction, and nozzles for greater spray coverage have organised this effort [7].

Technology, especially smart gadgets, sensors, and intelligent machinery, can reduce farmers' workloads. Aerial photography, GPS, temperature, and moisture sensors enable crop monitoring, mapping, and autonomous spraying. By using sophisticated technology, robotic systems, and precision agriculture, the agricultural sector may achieve a paradigm shift that increases profit, safety, efficiency, and sustainability [8, 9]. Modern technologies including UAV surveillance and pesticide spraying, image analysis, and spraying nozzle optimization are used in this work to improve crop number, quality, and farmer revenue.

AI and machine learning are revolutionising agriculture and will effect global markets [10]. Soil, water, agricultural, and livestock management can be improved through machine learning. AI can optimize a fixed area's yield for profit. AI can increase plant disease, weed identification, and harvest quality [11]. AI transforms agriculture by increasing farm production, GDPs, food security, and the environment. Agriculture uses artificial methods like crop monitoring, yield optimization, soil optimization, irrigation, and pest management.

Agriculture must be revolutionised in a world where technology is changing everything. Thus, UAVs transform agriculture. From spreading seeds to spraying pesticides, UAVs can optimize agriculture operations, monitor crop growth, and boost crop production [12]. Plant health and pests are monitored using surveillance UAVs. UAVs with AI also assess soil moisture, fertility, and other parameters that affect plant development. As the country's population grows and weather patterns change, farmers must adapt to new technologies [13]. By monitoring farms using UAVs, UAVs increase traditional farming's quantity, quality, and revenue.

1.1. Objectives of the Research. As discussed earlier, the development of stable and economical UAVs is very essential for small- and medium-scale farmers in India. A plethora of literature is available on UAV technologies, but there are still gaps available to overcome those issues. Hence, the objectives of this work have been formulated to address the following issues: (1) Endurance is dependent on the overall weight of the UAV. This work has been designed to cover 1 acre of agricultural land in 10 minutes by carrying a pesticide of 10 litres. The frame contributes mainly to the overall weight of the UAV. Hence, the reduction of frame weight to increase endurance while maintaining the payload of 10 kg is the primary objective of this work. (2) Precision spraying is one of the important factors to be considered for reducing not only the cost but also the environmental pollution. Hence, the development of an AI-based crop health condition monitoring system is another objective of this research. And (3) comparing the crop yield of customized UAV-sprayed paddy crop with manually sprayed paddy crop.

1.2. Related Works. This section divulges about the literature review for the current work, based on the input from the previous work on applications of AI in agriculture, smart farming, design and analysis of hexacopter, usage of UAVs in agricultural applications, selection of suitable UAV components, and spraying nozzle design optimization and calculations which are used for this study. The importance of artificial techniques in agriculture was investigated. Agricultural automation is of high concern as the traditional techniques followed by farmers are not sufficient to fulfil the food requirements of the increasing population. This paper has audited the applications of artificial intelligence in agriculture for weed removal and spraying using UAVs. The usage of UAVs is also discussed in spraying applications and crop monitoring. The comprehensive information is listed in Table 1.

Yallappa et al. [24] designed a hexacopter agriculture spraying UAV with a 15-minute flying time, 2 km range, and 1.5-litre fluid capacity. Selection and computation of components were done. The authors attached a GoPro video camera to photograph and monitor the spraying mechanism. Yeong and Dol [25] researched the computational and experimental test-based effective outcomes of multirotor UAV. Both engineering approaches examined the multirotor UAV's rotors. The multirotor UAV propeller's initial design phases were revealed, wherein thrust-to-weight ratio, typical multirotor UAV configuration, and number of propellers involved in important lifting phases were presented. Analytical propeller construction methods are the main focus of this work. Raja et al. [26] conceptually created the multirotor UAV for environmental applications, providing analytical methodologies for developing all UAV components. Design ratio, fineness ratio, and their roles in multirotor UAV building were highlighted. The ideal values for both ratios were mentioned. These ratios, their proper values, and known design criteria made comprehensive design processes easy to achieve. Analytical methodologies for secondary design parameters (thickness) of connection arms and landing sticks were explored in addition to fundamental design parameters (length and diameter). Suprapto et al. [27] examined the design viewpoint of a heavy payload hexacopter for diverse purposes. The component sections and their subordinate analytical approaches were discussed. Through this effort, components other than propellers could be selected. In particular, the propeller-motor-battery-electronic speed controller-flight control board connections were indirectly implemented. The necessity of initial weight estimation and its final optimization was also emphasised. Due to the substantial payload-based application, these analytical methodologies and shortlisted components complement the current effort.

Lack of available workforce for agricultural production activities is one of the most pervasive problems that farmers face today. This issue will continue for the foreseeable future because the next generation does not have enough opportunities to choose from in terms of employment fields. Manual sprayers of pesticides are putting their health in danger since they are exposed to the poisons they employ on the job. UAV technology has a wide range of possible uses in

Table 1: Investigations on UAVs and components selection.

Specifications	Description	Investigators
Autonomous spraying UAV	Agricultural UAVs help in increasing yield and crop growth	Garre and Harish [14]
UAV in agriculture	UAVs integrated with cameras are the prominent requirement as the images are used in weed identification, soil analysis, and monitoring	
Security of distributed intelligence in edge computing	The impact of UAV combines with data privacy, device security, and secure communication	Chen et al. [15]
Challenges in smart agriculture	Remote range, data storage and transfer, signal interference, and UAV implementation in all fields are some of the challenges	Maddikunta et al. [2]
Nozzle spray applications	To understand the droplet and spray pattern in the agricultural UAV	Psirofonia et al. [16]
Spray characterization of flat fan nozzle	Perform evaluation of flat fan nozzle under various drifting conditions	Guler et al. [17]
Crop monitoring	Linear regression method for sunflower crop	Vega et al. [18]
UAV nozzle spray droplet size	Understanding the spraying droplet spectrum varying the speed and height of spraying	Martin et al. [19]
Spraying efficacy	Effective ways of utilizing UAVs for increasing spray efficiency and efficacy	Liao et al. [20]
Crop monitoring	Mapping, image processing, and comparison study have been conducted	
UAV computing	UAV-assisted autonomous search and rescue system for disaster response	Huang et al. [21]
Spraying fertilizers and pesticides	It has the ability to reduce time and human effort	Pharne et al. [22]
Context of industry 5.0 in UAV in agriculture	Industry 5.0 and precision agriculture	Gomes et al. [23]

agriculture and provides a stable system on which to operate. UAVs that can carry more weight are the subject of constant interest and development. UAVs have several advantages over more traditional farming tools and techniques, especially for large agricultural plots. In the field of agri-UAVs, there is a deficiency of agricultural and scientific data necessary to determine which UAV parts are most applicable. Another major challenge is gathering enough images to use in training artificial intelligence systems for use in precision farming. There is potential for the development of low-cost UAVs with a high payload capacity that can be used to spray a wider area. Choosing the right spraying nozzles to cover large areas reduces not only the operational costs but also the amount of pesticide needed to perform the job. Field trials of a spray to determine its quality and efficacy require knowledge of the best spraying system to utilize for each crop variety. It is important to remember that research into spray droplet deposition and area coverage, spray drift management, and its impact on crop output is in its infancy and has yet to be applied to a wide variety of crops and locations. It is also important to stress the fact that this study is just getting started. There is a paucity of UAV testing facilities for evaluating its various parts. The furthermore comprehensive highlights are listed in Table 2.

2. Design and Development of Lightweight, Heavy Payload Hexacopter

The number of times that UAVs are being put to use in agricultural settings is rapidly increasing. Nevertheless, there are constraints, some of which include, but are not limited to, cargo capacity, thrust of the UAV, endurance, controllability, operational cost, and safety of operations [28]. In this context, both the quadcopter and the hexacopter find widespread application in the field of precision agriculture [29]. Despite the fact that both are put to significant use, the quadcopter has a number of drawbacks, including poor payload capacity, instability, and a high risk of crashing even if just one of its propellers stops working [30]. According to Suprapto et al. [27], however, hexacopter has improved payload lifting capacity while also preserving efficiency and providing better stability. In spite of the fact that the hexacopter has a lower endurance than the quadcopter due to the additional two motors, the hexacopter was selected for this investigation because of its superior stability. Due to the fact that we have extensive experience in the field of spraying, it was agreed that the new hexacopter should have the characteristics detailed in Table 3.

Since the commercially available hexacopters are heavy and expensive as discussed in [31], it was decided to design, manufacture, and assemble the hexacopter to make it affordable and lightweight. Since the majority of the UAV performance indicators are dependent on weight, the major focus is given to the reduction of weight in frames, arms, and fuselages, whereas propeller shafts, motors, and batteries were purchased based on our requirements.

2.1. Overall Take-Off Weight Estimation. The performance of a hexacopter is mainly dependent on the ratio between overall weight to payload. This ratio is very essential to calculate the flight parameters such as thrust, power, speed, and endurance of which thrust is the major factor that needs to be calculated. It is noteworthy to mention the fact that all the commercially available hexacopters have W_O/W_p, and it

Table 2: Comprehensive summary of the highlights.

Sl no.	Objectives defined	Outcomes
1	Endurance is dependent on the overall weight of the UAV. This work has been designed to cover 1 acre of agricultural land in 10 minutes by carrying a pesticide of 10 litres. The frame contributes mainly to the overall weight of the UAV. Hence, the reduction of frame weight to increase endurance while maintaining the payload of 10 kg is the primary objective of this work.	A UAV with a 20% reduction in weight was achieved to carry a 10 kg payload and it helped to increase the endurance by 2 min.
2	The nozzle of the sprayer plays a vital role in the efficiency and the crop yield. Hence, the selection of a nozzle covering a large area is another objective of this research and experimentally validated in the lab and in the crop yield.	A correlation between the nozzle and the area coverage has been established for different nozzles. Recommendations for the selection of nozzles for 5 different plants which are widely cultivated in India are given.
3	Precision spraying is one of the important factors to be considered for reducing not only the cost but also the environmental pollution. Hence, the development of an AI-based crop health condition monitoring system is another objective of this research.	Three different AI algorithms were tested and found that CNN was more effective as compared to other algorithms in identifying plant health with less computational time.
4	Comparing the crop yield of customized UAV sprayed paddy crop with manually sprayed paddy crop.	UAV-based spraying has increased the crop yield by 0.4 tons per acre while the reduction in spraying cost by INR 200 per acre.

Table 3: Hexacopter design parameters.

Design data	Parameters
Payload	10 kg
Endurance	10 min
Operating speed	3 m/s to 6 m/s
Range	2 km
Mode of flight	Manual and autonomous

was decided to develop a lightweight hexacopter with W_O/W_p ratio between 2.4 and 2.8. Although it was designed to carry 10 kg of liquid fertilizer or pesticide, it is also essential to include the weights of the spraying tank as well. Therefore, the payload needs to be calculated as given in the following equation:

$$W_{\text{Payload}} = W_{\text{Primary}} + W_{\text{Secondary}}, \tag{1}$$

where

$$W_{\text{Primary}} = W_{\text{Tank+pesticides}} \Rightarrow W_{\text{Primary}} = 10.74\,\text{kg}. \tag{2}$$

The high-density acrylonitrile butadiene styrene (ABS) plastic material was selected for the pesticide tank as it is economical compared to metal and composite materials [32]. The tank was designed as shown in Figure 1.

$$W_{\text{Secondary}} = W_{\text{Nozzle}} + W_{\text{Pump+supportingrods}}. \tag{3}$$

The nozzle is one of the most important components in the agricultural UAV. Nozzles are used to spray fertilizers/pesticides on agricultural land. A motor pump is used to pump the fluid from the tank to the nozzles. The spraying quality in agricultural land with the help of nozzles is one of the objectives of my research. The weight of the nozzles measured is 0.040 kg.

$$W_{\text{Nozzle}} = 0.040\,\text{kg}. \tag{4}$$

The supporting components such as connecting rods or sticks, wireframe model-based platforms, truss structured-based connecting plates, and motor pumps are always predominant in the holding of payloads and their execution. For this work, four connecting sticks are used to hold the storage tank and nozzle setups with the main hexacopter. Thus, the major weight of the supporting components of this UAV comprises the weight of the sticks.

$$W_{\text{Pump+rods}} = 0.67\,\text{kg}. \tag{5}$$

Therefore, the consolidated weight of the secondary payload is calculated with the help of the following equation [33]:

$$W_{\text{Secondary}} = W_{\text{Nozzle}} + W_{\text{Pump+rods}} \Rightarrow 0.04 + 0.67 \Rightarrow 0.71\,\text{kg}. \tag{6}$$

After the estimation of secondary payload weight, the estimation of the overall weight of the payload needs to be calculated. In this regard, the equation [34] is referred to

$$W_{\text{Payload}} = W_{\text{Primary}} + W_{\text{Secondary}} \Rightarrow 10.74 + 0.71 = 11.45\,\text{kg}. \tag{7}$$

In this work, it was arbitrarily decided to have W_o/W_p at 2.4 for a given payload of 11.45 kg. As W_o/W_P of commercially available UAVs are in the range of 2.4 to 2.8, it was decided to design the proposed system to have W_o/W_p at 2.4 as it provides low weight and subsequently offers better endurance. Therefore, the maximum required overall weight was calculated as per the following equation:

$$\frac{W_{\text{Overall take-off}}}{W_{\text{Payload}}} = 2.4, \tag{8}$$

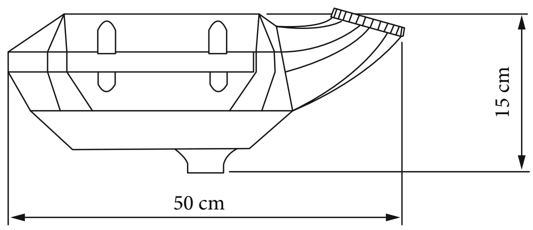

Figure 1: Spraying storage tank.

$$W_{\text{Overall take-off}} = W_{Payload} * 2.4 = 11.45 * 2.4 = 27.48\,\text{kg} \approx 28\,\text{kg}. \tag{9}$$

2.2. Calculation of the Diameter of the Propeller. The propeller is the only thrust-producing component in the UAV [35]. It transforms rotary motion produced with the help of a motor into linear thrust. It produces lift by the difference in the pressure between the top surfaces and bottom surfaces of the propellers. The variation of the speed of the propellers results in changing the direction of the UAV into roll, pitch, yaw, hover, take-off, and landing. Based on the configuration, the numbers of propellers vary. UAV propellers usually come with six in the case of hexacopter. The materials of the blades are carbon fibre or plastic. Plastic propellers are more flexible and less durable than carbon fibre. Carbon fibres are light in weight compared to plastic, and they also reduce the vibration caused due to rotation of blades [36]. Propellers are manufactured with two specifications. First is the length of the propellers also called as the diameter of the propeller. If the length of the propeller is small, inertia will be less, so less energy is required to spin them, and it is easier to control their speed [37]. The longer the length of the propeller, the more lift is produced with good stability, but it consumes more power. Second is the pitch of the propeller. The pitch of a propeller is defined as the distance moved for one revolution of a propeller. If the pitch is smaller, it will be stable, and hence the speed will be less compared to high-pitch UAVs. High-pitch UAVs will fly faster for a particular RPM but they consume more power. Since manufacturing of propeller is expensive, it was decided to purchase a suitable propeller. Therefore, it is essential to calculate the thrust which is directly proportional to the overall weight of the UAV. Since a hexacopter has 6 propellers, the weight will be equally distributed and the thrust required for each propeller is calculated as given in the following equation [25]:

$$T_{\text{Propeller}} = \frac{[T/W_{\text{ratio}}] * [W_{\text{Overall take-off}}]}{n}, \tag{10}$$

where $T_{\text{propeller}}$ is the thrust requirement by a single propeller in kg, T/W_{ratio} is the thrust-to-weight ratio, and n is the total number of propellers. Therefore, the thrust required by each propeller is calculated as 9.33 kg.

$$\begin{aligned}\text{Thrust requirement by the single propeller} &= \frac{[2] * [28]}{6} \\ &= 9.33\,\text{kg}.\end{aligned} \tag{11}$$

It is important to mention that the higher the thrust-to-weight ratio will offer better controllability. Generally, the minimum thrust-to-weight ratio for agricultural UAVs is 1 : 2 to perform all kinds of aerodynamic maneuvring and to hover at half the throttle [38].

From the thrust requirement, the diameter of the propeller can be calculated using Equation (12) based on the momentum theory.

$$T = 0.5 * \rho * A * \left[(V_{\text{UAV}})^2 - (V_0)^2\right](N), \tag{12}$$

where ρ is the density of the air, 1.225 kg/m^3 at ambient temperature, A is the area of the rotational propeller, m^2, V_{UAV} is the velocity of air accelerated by a propeller, 24 m/s, V_O is the velocity of the air at the propeller, 5 m/s, and T is the thrust, $9.33\,\text{kg} * 9.81\,\text{m/s}^2 = 91.52\,N$.

$$0.5 * \rho * A_{\text{rotor}} * \left[(24)^2 - (5)^2\right] = 91.52 \Rightarrow A_{\text{rotor}} = 0.27\text{m}^2. \tag{13}$$

After that, the needful design data was estimated. The diameter of the propeller is equal to 0.58 m (23 inches). Hence, the propeller having a diameter of 23 inches will provide the required thrust.

2.3. Calculation of Pitch of the Propeller. Under the design consideration of the propeller, the pitch of the propeller plays a vital position along with the diameter. There were twenty propeller profiles used for agricultural UAVs that are available in the market were collected, and the relationship between various propellers to pitch by diameter (P/D) ratio is derived. From the second historical relationship, it is observed that most of the pitches to diameter fractions are located in the range between 0.35 and 0.40. In this work, P/D was arbitrarily chosen as 0.375 and the pitch was calculated as given in the following equation:

$$\frac{P}{D} = 0.375, \tag{14}$$

$$\begin{aligned}\frac{P}{23} &= 0.375 \Rightarrow \text{pitch}[P] = 0.375 * 23 \\ &= 8.6 \Rightarrow \text{pitch}[P] = 8.6\,\text{inches}.\end{aligned} \tag{15}$$

There are over 20 different propeller blades available of which foldable fixed pitch propeller blade provides better thrust performance [39]. Hence, in this work, a foldable fixed pitch blade was chosen, and its dimensions as depicted in Figure 2.

Based on various propeller design considerations, the estimated specification of the proposed hexacopter is shown in Table 4.

2.4. Estimation of Power Requirement. Estimation of power required by each propeller is very essential in choosing motors and batteries. The maximum power required for

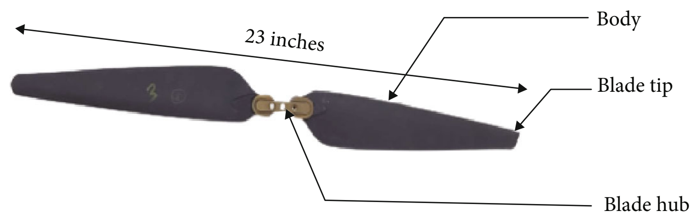

Figure 2: Propeller specifications.

Table 4: Calculated final design data.

Sl. no.	Description	Design data
1	Thrust by the propeller	9.33 kg
2	Thrust-to-weight ratio	2
3	Diameter of the propeller	23 inches
4	Pitch of the propeller	8.8 inches

100% throttle is calculated using Equation (16) as given by [26]

$$\text{Power} = \frac{1}{2} * T * V * \left[\left(\frac{T}{A * V^2 * \rho/2} + 1 \right)^{1/2} + 1 \right], \quad (16)$$

where T is the thrust by a single propeller and V_{UAV} is the velocity of air accelerated by the propeller, 24 m/s.

$$\begin{aligned} \text{Power requirement} = {} & \frac{1}{2} * 91.52 * 24 \\ & * \left[\left(\frac{91.52}{0.261 * 24^2 * 1.2256/2} + 1 \right)^{1/2} + 1 \right] \\ & \Rightarrow 1098.24 * 2.41 = 2646.7\ W. \end{aligned} \quad (17)$$

The maximum power required for 100% throttle is estimated as 2.6 kW. Although the hexacopter is designed to work with 50% throttle, it is essential to choose the power supply for 100% throttle condition in order to overcome surges and abnormal conditions.

2.4.1. Battery. The battery power is calculated by using Equation (18), and also battery consumption will be maximum while hovering over the aircraft.

$$\text{Flight time} = \text{battery capacity} * \frac{\text{discharge}}{\text{average ampere draw}}. \quad (18)$$

In the hovering condition, the lift of the UAV is the weight of the UAV, and the thrust required for hover per motor for full load condition is the total weight of the UAVs/no.of rotors, ⇒28/6 ⇒ 4.66 kg/motor.

From the generalized motor data sheet, the current required for generating 4.66 kg thrust is approximately 13 A. During full load hovering condition for lifting 1 kg of thrust, the current required is = 13/4.66 ⇒ 2.78 A to lift 1 kg; average ampere draw = current required to lift 1 kg of load ∗ overall weight ⇒ 2.78 ∗ 28 = 77.84A. Since estimated flight time is assumed as 10 mins = 0.16 hours, 0.16 = battery capacity ∗ 0.8/77.84 ⇒ battery capacity = 15.568 Ah. A battery of 15.568 Ah is required for 10 mins endurance; in this work, six cells, lithium polymer (LiPo) battery with 16000 mAh (16 Ah) battery of TATTU make was used.

2.5. UAV Frame Design. Since a hexacopter has 6 arms, each arm needs to be placed in equidistance. Simply, each arm needs to be separated by 60°. The length of the arm is dependent on the length of the propeller. Clearance between tip to tip of the propellers decides the arm length of a UAV [40]. Based on these requirements, in this work, an arm length of 65 cm was chosen. Since this work is fully dependent upon the conventional design of hexacopter rotor-based multirotor UAV, the estimation of angle representations of all the connecting arms can be derived from the help of simple geometry. Thus, it is observed that the assembling of connecting arms is predominantly arriving at the equilateral triangle, as shown in Figure 3. In Figure 3, the central hub of the UAV is referred to as "X" and "Y" and "Z" are referred to as positions of the propeller mounts of two different motors in which the distance between the hub is shown as A and B, respectively. As stated, the angle between each arm of the rotors is 60° and the length of the arm is 65 cm, and this data clearly results that for the hexacopter, the length of the arm should be equal to the distance between the hub of the motor which is mentioned as C. So, $A = B = C = 65$ cm.

So, lengths of all the connecting arms and distance between the motors should be equal. The frame size ranging from 600 mm to 1200 mm is used for agricultural UAVs. With the study on the existence of the agricultural UAV, frame size is designed. The proposed arm model is shown in Figure 4.

2.6. Selection of Fuselage. The selection of fuselage for UAVs has been generally relayed on two factors: the external boundaries of electronics equipment and the enclosure and shape of the fuselage. Since the outer shape of the fuselage is one of the main factors in generating the drag force on the entire multirotor UAV, the shape of the multirotor should be always kept as curvature-based instead of bluff body orientation. Based on the commercially available shapes and materials, in this work, ABS was used due to its cost and relatively low weight. The fuselage used in the work is shown in Figure 5.

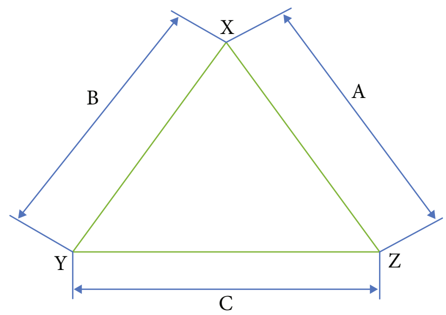

Figure 3: The trigonometric representation of the UAV frame's design.

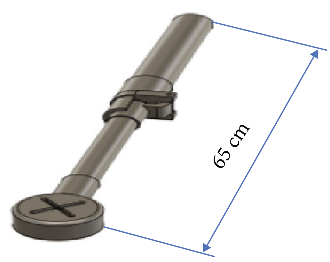

Figure 4: Isometric view of connecting arms.

By selecting the appropriate commercially available components and custom-made arms, the UAV was assembled. The assembled UAV is shown in Figure 6. The weight of the assembled UAV is 26 kg which is 2 kilos lower than the anticipated weight discussed in the earlier section. Further, the weight is lower than the commercially available UAVs. It is noteworthy to mention that the cost of the assembled UAV is nearly 30% lower than the commercially available UAVs.

3. Deep Learning Embedded for Crop Monitoring

As the usages of UAV are increasing, it is essential to make it for precision farming. First, UAV is responsible for mapping the large-scale agricultural area which in the current work is a rice field, lemon, and guava field located in Kumaraguru Institute of Agricultural, Satyamangalam, Tamil Nadu, to get the coordination of the area boundaries by using GPS to get location data in latitude and longitude format. It is one of the objectives to understand the leaf condition through image processing techniques. It has been decided to focus on a lemon and create a dataset for a lemon. In India, lemon has been cultivated 3.17 lakh acres in which India contributes 17% of the world's lemons [41]. Despite it has been cultivated in large volume, to our knowledge, the dataset for lemon leaf is limited. Therefore, in this work, a dataset of lemon cultivation land was created by photographing with a gimbal camera and DSLR camera. The image dataset having 838 unhealthy and healthy lemon leaf images was created by capturing the images. The images were taken from the land owned by Kumaraguru Institute of Agriculture wherein 1 acre of land was used to cultivate

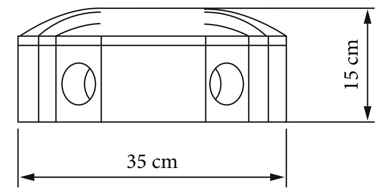

Figure 5: Front view of a fuselage.

Figure 6: Isometric view of the assembled hexacopter.

lemon. The dataset of lemon leaf captured was analysed using three different algorithms to classify the stress level of the leaf. In this work, logistic regression, random forest, and convolutional neural network (CNN) algorithms were used to classify and identify the stress level of the leaf to spray the pesticide effectively. Since this is a new dataset, in this report, AI-based disease identification and classification of lemon leaf is only presented in this report [42].

3.1. Hexacopter with Gimbal Camera. In the present study, a hexacopter with a gimbal camera is used for mapping and taking images of the crop land. Existed hexacopter design was chosen for the study and performed the comparative study on choosing the gimbal camera and fitting it in the UAV. Table 5 contains the hexacopter specifications.

3.2. Gimbal for Camera Stabilization. Various factors distinguish cameras, but the most significant for photogrammetric applications are optics quality, sensor quality, and lens compatibility. A gimbal is a supporting mechanism that allows the camera to remain in the same position. By automatically adjusting using calibrated and typically remotely controlled electric motors, a gimbal can control the movement of the camera independent of the movement of the UAV. Gimbals dampen vibration in UAVs, which is extremely useful for real-time picture stabilization applications and gives advantages for capturing better pictures. Gimbals usually have two or three axes. Images captured in 2-axis gimbals will have significantly greater roughness as they do not correct for yaw. A three-axis gimbal provides additional stability by managing the camera's yaw movement. A three-axis gimbal is used in the current research. The proposed hexacopter UAV with a gimbal camera is shown in Figure 7.

In this, the proposed hexacopter with a gimbal camera is used to map the agricultural land. The samples of the images of the leaves are shown in Figure 8. The leaf dataset is gathered and subsequently processed for the assessment of the leaf's health state using appropriate algorithms.

Table 5: Proposed hexacopter specifications.

Major components	Specifications
Sensor units	
BLDC motor	1400 KV
Electronic speed controller	30 A
Thrust-to-weight ratio	1 : 2
Gimbal	3 axis
Flight control board	Pixhawk 2.4.8
Frame	550 mm * 550 mm * 100 mm
Maximum speed	25 m/s
Range	2 km
Power unit	
Battery	8000 mAh
Operating time	12 min
Propeller unit	
No. of propeller	6
Operational mode and weight	
Net weight	2 kg
Operational mode	Autonomous/manual

Figure 7: Developed hexacopter UAV with gimbal camera.

3.2.1. Procedure to Process the Images. The data collected by the hexacopter UAV is stored and processed by following the steps shown in Figure 9. This storing system allows the user to access data from any location and at any time. For simple access, the image data is saved with the name and time of capture. For crop health analysis, the recorded photos are analysed utilizing image processing and the proposed algorithms [43].

3.2.2. Leaf Images. Leaf images are the input images, whose health has to be analysed to check the stress level and health condition of the leaf. This image was processed by following the steps.

(1) Preprocessing. At this stage, the input images are preprocessed to speed up the process and reduce the computational and memory complexity in the cloud. Here, two steps are followed to perform a preprocess on the input images. The steps are as follows:

(a) Image resizes

In this step, the input image size is resized into $250 * 250 * 3$ to reduce the computational complexity. In this work, the input image size is $256 * 256 * 3$. This size is reduced to $250 * 250 * 3$ for processing all types of images in the future. This resized image is subjected to color transformation to highlight the healthy and unhealthy regions in the leaf.

(b) RGB to BGR conversion

In this step, the input RGB channel of the image is converted into a BGR channel to signify the healthy and unhealthy regions of the leaf using the following algorithm 1 [43]. Using algorithm 1, the HSV plot for the RGB and BGR image is shown in Figure 10 [43].

Figure 10 shows that the blue and red channels are interchanged to highlight the healthy regions of the leaf. This highlighting helps to improve the segmentation process.

(2) Leaf Region Segmentation. At this stage, the final preprocessed image is processed to segment the leaf region from the background image. It is achieved by two stages of masking. One is green masking to segment the healthy regions, and the other is brown masking to segment the unhealthy regions. By combining both this stage's output, the leaf region is extracted from the background and it is useful for efficient classification.

(a) Healthy region

In this, the healthy region of the leaf is extracted by defining the pixel range for the upper and lower parts of the leaf. The combined upper- and lower-part values give the mask for extracting the healthy region of leaves. Algorithm 2 is for healthy region segmentation [43]. Using algorithm 2, the healthy regions of the leaf are extracted, and they are shown in the result section [43]. This segmentation helps to improve the feature extraction and classification process.

(b) Unhealthy region

Similarly, by setting the pixel range for the top and bottom regions of the leaf, the unhealthy region of the leaf is retrieved. The mask for removing the unhealthy zone of leaves is created by combining the upper- and lower-part values. The method for segmenting unhealthy regions is shown in algorithm 3 [43]. The diseased parts of the leaf are extracted using the technique described in algorithm 3 [43], and they are displayed in the result section. This segmentation aids in the extraction and categorization of features.

(c) Final segmentation

In this, the outputs from both stages are combined to produce the final segmented leaf image from the background. The algorithm for the final segmentation part is shown. Using the

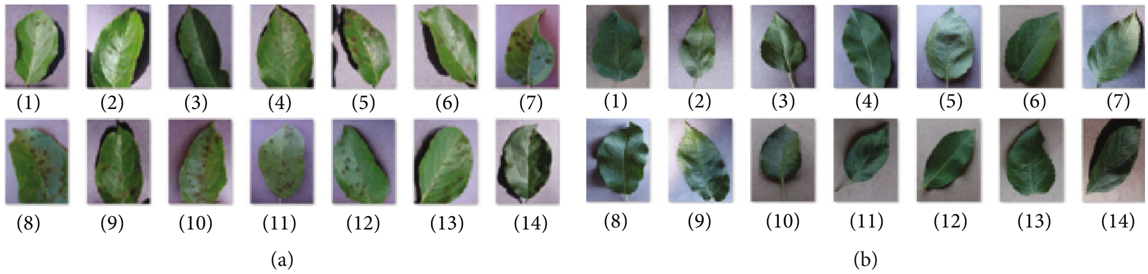

Figure 8: (a) Deceased leaf samples and (b) healthy leaf image samples.

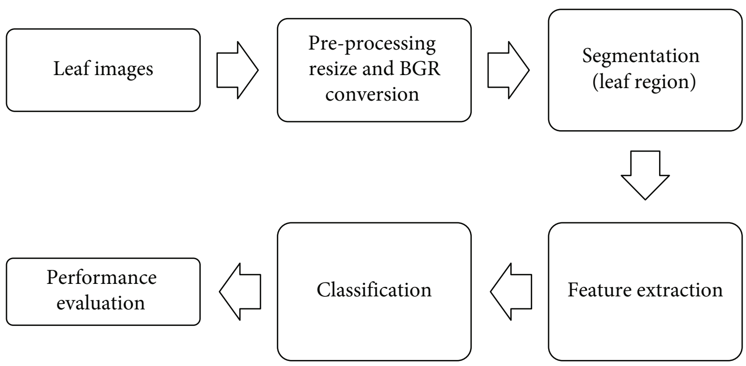

Figure 9: Steps for processing the images.

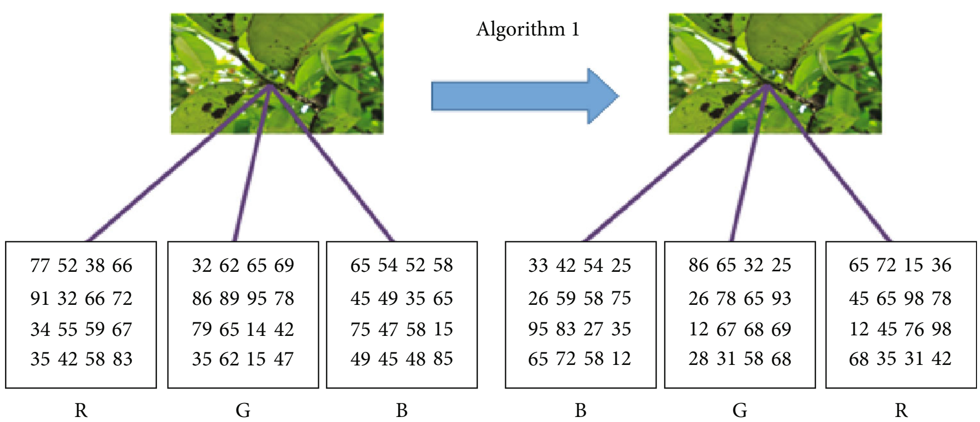

Figure 10: 2^{nd} stage of preprocessing output.

algorithm 4 process, the leaf region is extracted from the background image [43]. This extracted image is subjected to the feature extraction and classification process.

(3) Feature Extraction. In this step, the pixel count for each channel value is calculated for the leaf region, and it is called the histogram count. After calculating the histogram count, the normalized values of the image are also calculated. These two parameters are useful for performing classification using logistic regression and the random forest algorithm. Algorithm 5 is for performing the feature extraction process [43]. Using the algorithm 5 steps, the feature extraction is performed on the leaf region, and the corresponding results are shown in Figures 11 and 12 [43].

In Figure 12, the x-axis indicates the pixel values and the y-axis indicates the number of counts in that pixel. This gives the histogram count of the image. From Figure 12, it is observed that the leaf region has a maximum pixel count of between 2 and 160. Based on the histogram count, it is observed that the maximum pixel value in the image is 160. Hence, the 160 is chosen as the normalization for the input image. Then, the corresponding normalized histogram image is shown in Figure 12.

Figure 12 shows that the histogram value is normalized to the range of 160. This improves the feature extraction by analyzing the regions more dominantly as compared to the histogram count of the image. Both these values are used for classification by a machine learning algorithm [43]. For

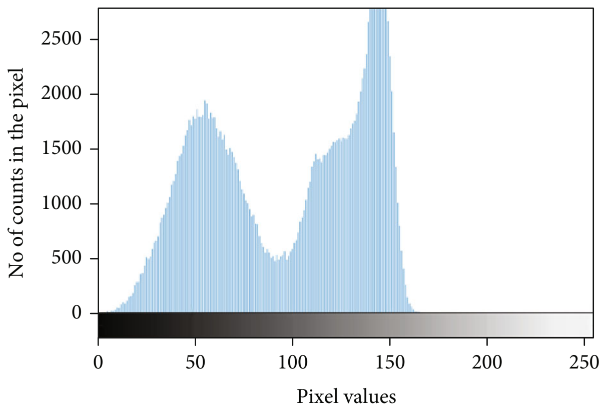

Figure 11: Histogram count.

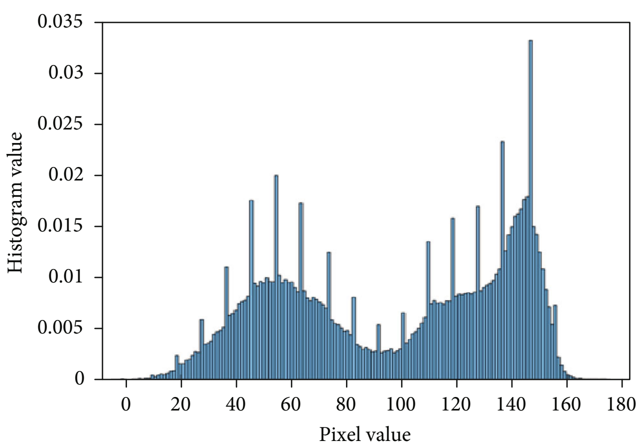

Figure 12: Normalized histogram count.

deep learning algorithms, the segmented images are directly processed instead of these extracted features [43].

(4) Performance Evaluation. In this section, the metrics used for evaluating the classification process are discussed.

(a) Accuracy

Accuracy is an evaluation metric for the classification process. It defines the classifier performance by identifying the leaf types correctly as shown in the following equation:

$$\text{Accuracy} = \frac{\text{correctly identified classes}}{\text{total number of classes}}, \quad (19)$$

$$\text{correctly identified classes} = \text{healthy or unhealthy type}. \quad (20)$$

(b) Computational time

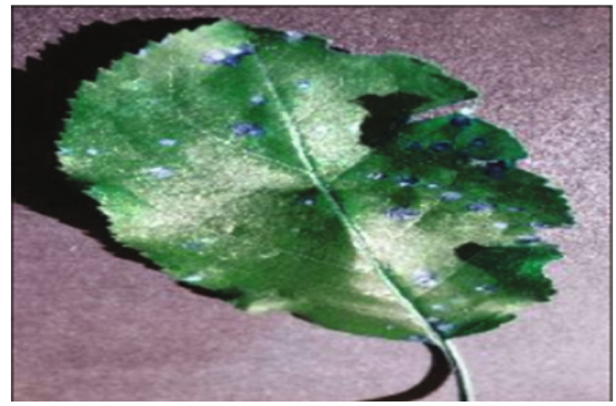

Figure 13: Resized image.

Computational time is the time taken to complete the image-processing task for each algorithm [43]. Generally, the computational time should be low for faster processing.

3.2.3. Surveillance Room. The manual operation settings for the UAV may be supplied in this room, and the UAV's motions can be watched to replenish the UAV's energy if it runs out. In this section, the output for each stage of image processing is shown, and the comparison of machine learning algorithms is given [43]. In this, the input image is resized to 250×250, and then it is transformed into the BGR domain to observe the changes in the leaf to indicate the type of disease, as shown in Figure 13.

The figure shows the sample resized image for processing on the UAV because the larger image size requires more space and processing time. Hence, in this, the (250, 250) size is chosen for processing all the images from the UAV. After resizing, the image undergoes color transformation using a relevant algorithm [43]. The output of color transformation is shown in Figure 14.

Here, it is observed that the RGB channel of the image is transformed into the BGR channel as in Figure 14(b). This transformation highlights the maximum changes in the leaf region.

(1) Segmentation. After the color transformation process, the leaf image is separated from the background using a segmentation algorithm [43].

Here, the segmentation is performed by two types of masking. One is green masking, and the other is brown masking. In green masking, the upper and lower regions of the leaf in green color are masked as in the first part of Figure 15. The second part of Figure 15 shows the leaf structure of the mask. Similarly, the second masking is performed, and its results are shown in Figures 16 and 17.

In brown masking, the unhealthy regions and stem regions of the leaf will be covered. In the input image, the brown images are fewer; hence, it shows a smaller white area in the first Figure 16 as compared to green masking. The corresponding output for the brown mask is shown in the second part of Figure 16. By combining both this green

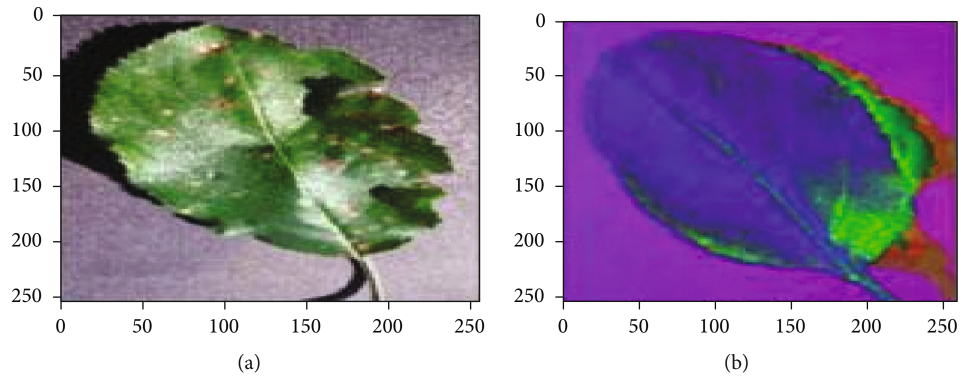

Figure 14: Color transformation.

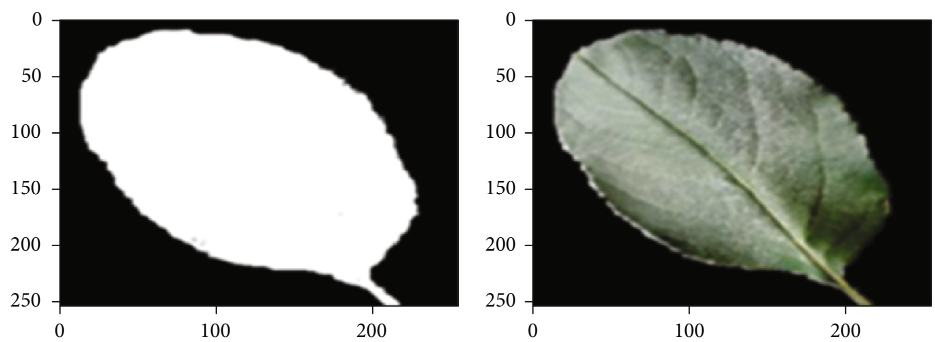

Figure 15: Green masking results.

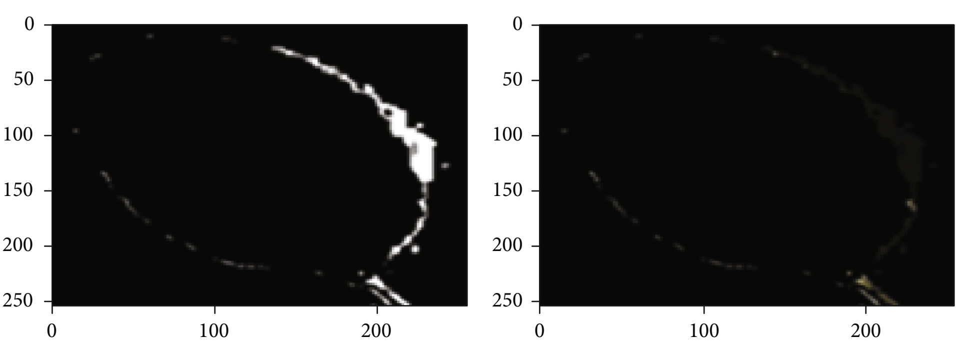

Figure 16: Brown masking results.

and brown masking, the complete leaf structure can be extracted from the background. Figure 17 shows the complete segmentation of the leaf from the images. The result shows that the proposed segmentation is suitable for extracting all the regions from the leaf as compared to other segmentation approaches like FCM or K-means that segment a single region into one part.

(2) Classification. From the segmented image, the deep learning algorithm is applied to it for feature extraction and classification purposes [43]. The performance evaluation of the deep learning classification for training and validation sets is shown in Figure 18. Figure 18 shows that the CNN performs well by increasing the epochs to reduce its model loss to a 0.10% value. Similarly, the corresponding validation loss is also minimal and falls under 0.05%. This proves that the proposed deep learning performance is individually better by having minimal loss as compared to the training set. Then, the overall validation accuracy for the trained CNN is shown in Figure 19.

Figure 19 proves that at higher epochs, the trained model can achieve 100% accuracy for properly trained CNN. This shows that the proposed deep learning algorithm is best for the dataset [43]. To verify this, the proposed method's performance is compared with the existing approaches like logistic regression and random forest in terms of computational time and epochs. The comparison between the proposed method and the existing method is given in Table 6.

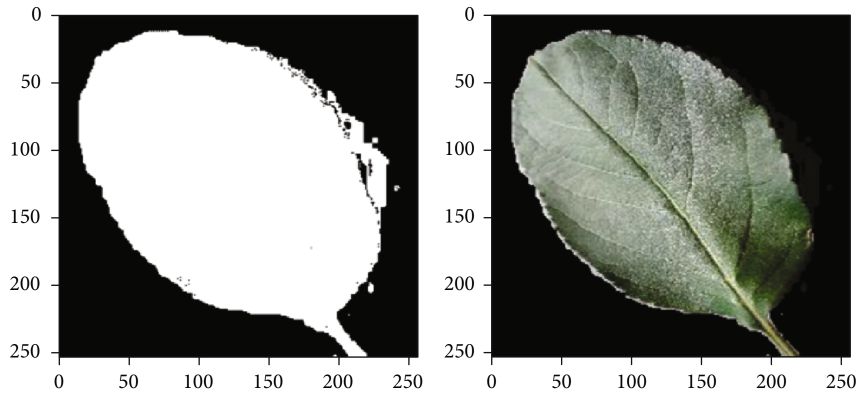

Figure 17: Final segmented result.

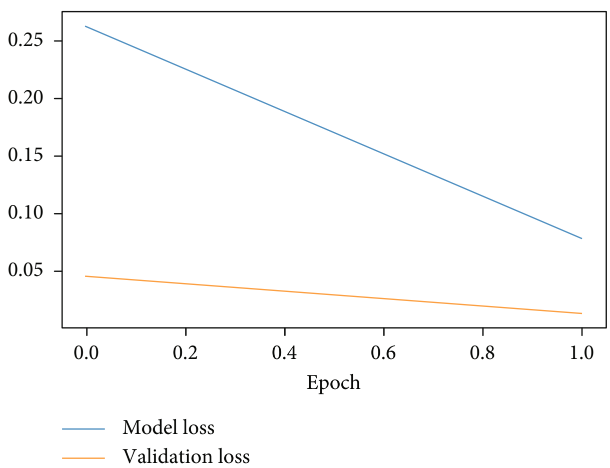

Figure 18: CNN evaluation.

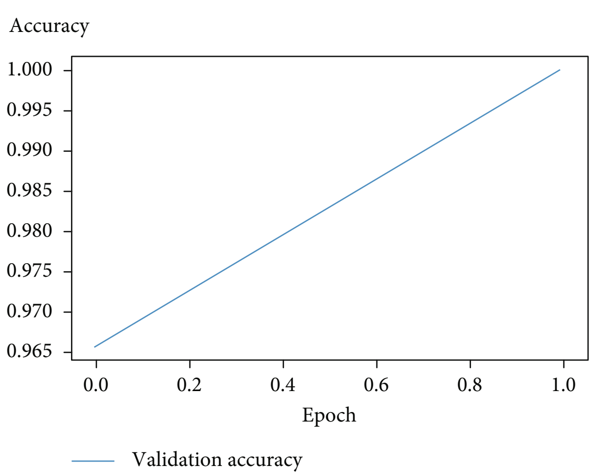

Figure 19: CNN validation accuracy.

From Table 6 and Figures 20 and 21 also, it is observed that the proposed method outperforms the existing method by having less computational time. From both the performance evaluation and the computational time, it is clear that the proposed deep learning is best for embedding in UAVs. The dataset of the lemon plant was created. It is found that CNN is the most powerful method yielding 99% accuracy and consuming 33% and 20% less time as compared with logistic regression and rainforest algorithms, respectively [43]. It is necessary to integrate this AI algorithm in the UAV for precision spraying of pesticides.

4. Experimental Validation of Thrust and Nozzle Spray Optimization

Two of the main objectives of this research work are to generate sufficient thrust at different flying conditions and develop a nozzle which covers a large spray area. Since we have estimated the overall weight of the hexacopter, it is necessary to test the thrust generated at different flying conditions such as take-off, landing, and hovering. Thrust measuring setup was created and measured the thrust by varying propeller, battery and motor [35]. In this chapter, the results of experimental validation of thrust are presented. Similarly, most of the conventional nozzles used commercially have limitations in spraying area coverage [44]. Nevertheless, it is crucial to spray the appropriate amount of fertilizers and pesticides at the right intervals in India, since the country possesses more than 157 million hectares of agricultural land and is a leading producer of rice, wheat, and vegetables [45]. Hence, it is very crucial to optimize on selection of a nozzle which can cover a large spray area. As part of this research, experimental results of custom-made nozzles are also provided in this section.

4.1. Thrust Measuring Setup. The thrust-to-weight ratio of a UAV varies depending on its applications [46]. As motors are propulsion systems for electric UAVs, they need to be chosen based on the RPM and KV rating of the motor. A motor with a suitable propeller will produce the required thrust. The thrust of the UAV is mainly controlled by varying motor specifications, propeller size, and battery [35]. The amount of thrust force decided the lift of the UAV. Therefore, a test setup to measure the thrust produced for different combinations was established in the laboratory, and the schematic is shown in Figure 22 and the thrust frame setup is shown in Figure 23. The experiments were carried out with a test bench fabricated using stainless steel to withstand the higher load produced by the motor.

Table 6: Proposed method comparison.

Methods	Accuracy (%)	Computational time (ms)
Logistic regression	65.3	175.5-1000
Random forest	82.7	150-900
Deep learning	98	55.96-748.34

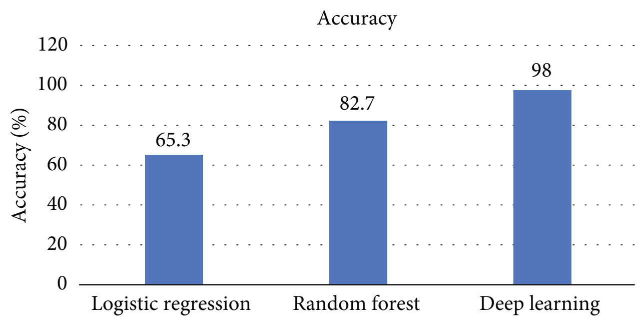

Figure 20: Accuracy comparison.

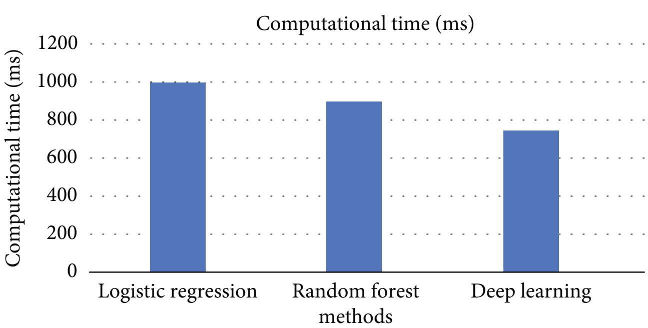

Figure 21: Computational time comparison.

The experiment involved utilizing an Arduino Nano in conjunction with a load cell to provide the measured data. The studies are undertaken to measure the thrust variation for different combinations of motor, battery, propeller, and ESC while manipulating the throttle. The importance of the load cell is to measure the propeller-induced aerodynamic force, the ESC is used to control the speed of the planned test propeller, and the control unit is used for guiding this entire experimental system. The experimental data is utilized to generate plots depicting the relationship between thrust and efficiency, RPM, power, and current under the given conditions.

4.1.1. Testing Procedure. Measuring the thrust for different speeds, motors, batteries, and propellers is essential to select the appropriate components for the proposed hexacopter. In this work, 6 propellers, 2 motors, and 2 batteries were used and tested for 40%, 50%, 60%, 70%, 80%, 90%, and 100% throttle positions. The process of testing of thrust measurement is depicted in Figure 24. LiPo battery is the only power source used in the testing setup. It is always important to check the voltage level of the battery for accurate readings, fix the propeller to the motor mount in the correct direction, and connect the motor and ESC to the battery. A servo tester is used to vary the speed of the motor and propeller setup. Note down the thrust produced, propeller RPM, and power consumed for each throttle position.

4.1.2. Experimental Results. Although this setup allows conducting different combinations, this work has been limited to two combinations, as shown in Table 7. The results were investigated between various parameters which include thrust vs. power efficiency, RPM vs. current, RPM vs. power, and thrust vs. RPM. These studies will provide a comprehensive idea of which system performs better and help to choose appropriate components for assembly.

(1) Results of Combination 1. Although experiments were conducted for two combinations, the results for one combination are provided here. The second combinations follow the same pattern. As anticipated, the consumption of power increases with increasing RPM, as shown in Figure 25. Since the speed of the motor did not increase linearly, there is a minor deviation in the linear relationship between RPM vs. power. Figure 25 also shows that the power consumption increases with increasing propeller length. At full throttle, the longest propeller consumed a power of 3200 watts, whereas the shortest consumed 2500 watts. Up to 80% throttle, all three propellers have the same pattern, and the longest starts consuming 20% more power for the throttle increased from 80% to 100%.

As power is dependent on the current, RPM vs. current followed the same pattern as RPM vs. power, as shown in Figure 26. The current consumed at 40% throttle for all three propellers was around 10 A, whereas in gradual increasing of throttle, a steep increase in current consumption is observed. By increasing the length of the propeller, RPM decreases, and the current consumption increases. The maximum current consumption for 100% throttle for 22-inch, 23-inch, and 24-inch propellers are 54 A, 61 A, and 72 A, respectively.

Similar to the previous cases, RPM vs. thrust showed increasing thrust for increasing RPM, and thrust generated was also increased for increasing propeller length, as shown in Figure 27. The 22-inch propeller can generate 10,000 grams of thrust at 7000 RPM. Comparatively, a 23-inch propeller can produce a better thrust of close to 12,000 grams at 6800 RPM, whereas a 24-inch propeller can result in a much higher thrust of exceeding 13,000 grams at 6400 RPM.

Power efficiency is defined as the ratio of thrust produced to the power consumed is one of the most important considerations in the selection of a propeller. Figure 28 shows the thrust vs. power efficiency, as anticipated, the 23-inch propeller performance was always in the middle between 22- and 24-inch propellers. Surprisingly, the 23-inch propeller exhibited superior power efficiency than the other 2 propellers, as shown in Figure 28. At the lower thrust, the power efficiency is between 4.4 and 4.5 for a 23-inch propeller which is reading just below 4.2 at the maximum thrust. In comparison, a 24-inch propeller and a

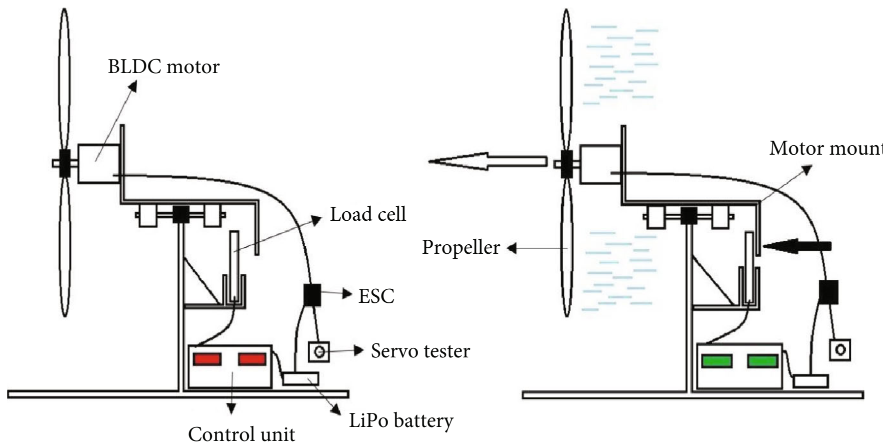

FIGURE 22: Schematic diagram of thrust measuring setup.

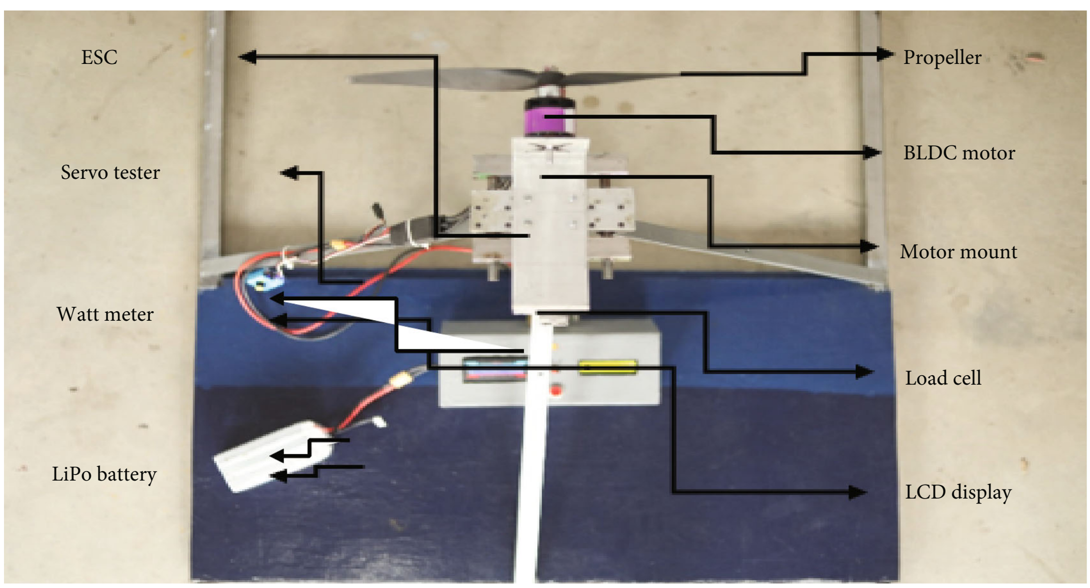

FIGURE 23: Thrust frame setup.

Step 1: check for the charge level of the battery that going to test

↓

Step 2: connect the motor, propeller, ESC to the battery.

↓

Step 3: make sure the propeller is fixed in the correct direction.
Avoid standing in front of the propeller.

↓

Step 4: gently increase the speed of the motor using servo tester.

↓

Step 5: note down the readings from the watt mater, tachometer

↓

Step 6: repeat the procedure by varying the speed of the motor

FIGURE 24: Process of thrust measurement.

Table 7: Variable combinations of UAV components.

Combination 1	Combination 2
Battery: 12 s	Battery: 12 s
ESC: 80 A	ESC: 40 A
Motor: 180 Kv	Motor: 320 Kv
Propeller: 22″ × 8.8, 23″ × 7.2, and 24″ × 7.9	Propeller: 15″ × 4.5, 16″ × 6.2, and 17″ × 5.5

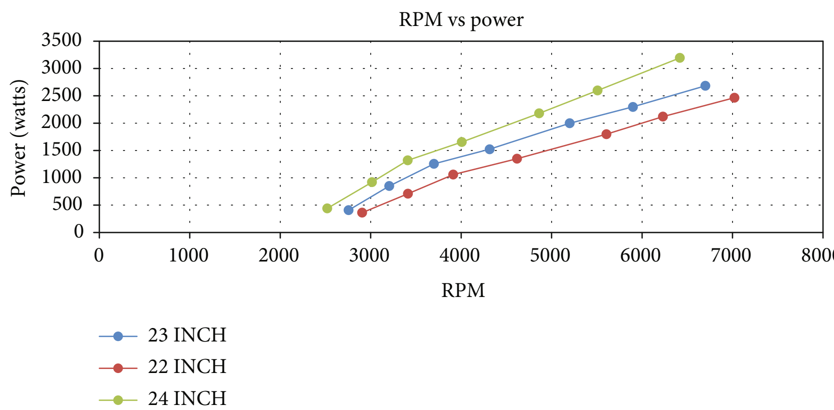

Figure 25: Comprehensive report between RPM and power.

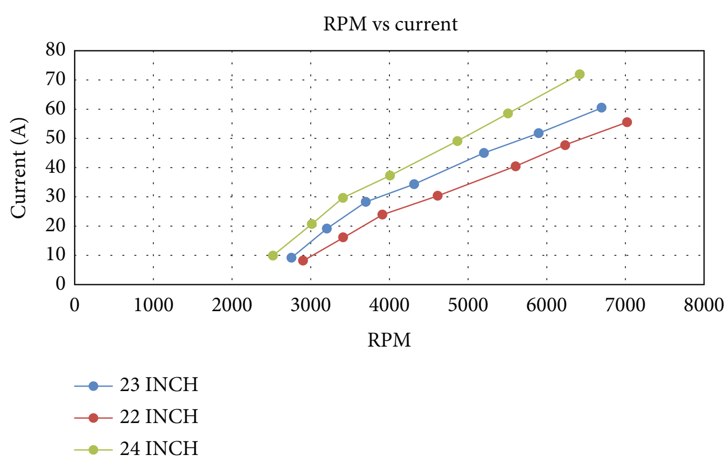

Figure 26: Comprehensive report between RPM and current.

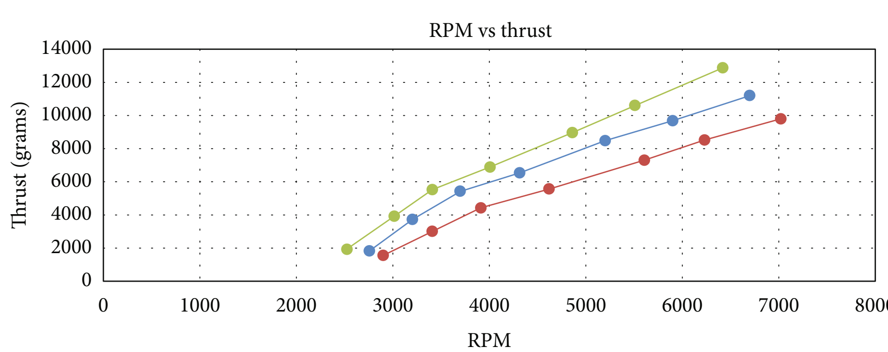

Figure 27: Comprehensive report between RPM and thrust.

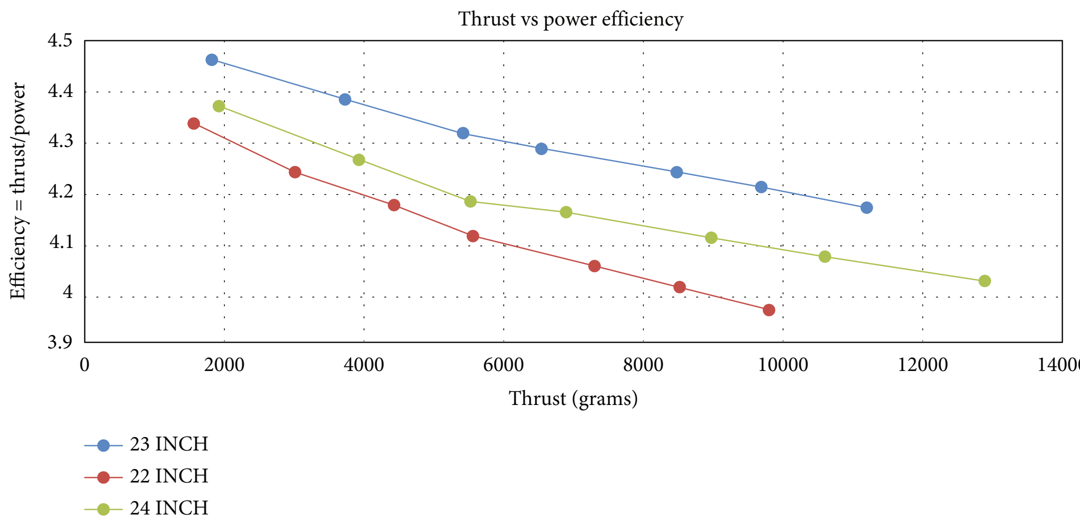

Figure 28: Comprehensive report between thrust and power efficiency.

22-inch propeller produce a maximum efficiency of 4.38 and 4.32, respectively, and drop to 4.03 and 3.97, respectively, at maximum thrust. The results show that the 23-inch propeller is best suited for the specified motor.

4.1.3. Field Study on Spraying Area Coverage and Time Consumptions. Since 3 m/s and 4 m/s are considered stable speeds for agricultural UAVs [19], tests were conducted to identify the time taken to cover 1 acre of paddy land and the area sprayed with a full tank capacity of 10 litres. The results of these experiments are given in Table 8. It is found that UAVs operated at 4 m/s cover a large area and consume only 6 minutes to cover an acre. However, both methods could not cover an acre of land with full tank capacity.

4.1.4. Manual Spraying vs. UAV Spraying. Two acres of paddy land were allotted on the premises of Kumaraguru Institute of Agriculture, Tamil Nadu. One acre was used for manual spraying and the other for UAV spraying, as shown in Figures 29 and 30. The type of crop and spray frequency are given in Table 9. The comparison of crop yield for both manual and UAV methods is given in Table 10. As anticipated, crops sprayed with UAVs yielded 16% higher than the manual method. Further, the usage of UAV reduced the operating cost by 50% for an acre as compared with manual mode.

The experiments conducted on thrust measurement suggested that a 23-inch propeller seems to be more power efficient for a given thrust. Although 24 inches performed better in most cases, in terms of power consumption, a 23-inch propeller is suitable for better endurance. Based on the experiments, recommendations on the selection of nozzles, orifice diameter, and the height of the spray are given in Tables 8–10. Since the required cone angle is between 80° and 110°, the suitable operating pressure is 4 bar. However, depending on the pesticides or herbicides, the pressure can be fixed. Despite the fact that the cone angle is expected to be between 80° to 110°, for better application of chemicals, in select cases, it is expected to operate at low pressures. For example, herbicides need to be sprayed at between 2 and 3 bar. Flat fan nozzles are recommended when the spray has to be percolated to the bottom, whereas full cone nozzles are recommended for shallow penetration. For instance, paddy is a crop where the stems are thin but dense crop, in such cases flat fan is preferred so as to reach the inner surfaces of the stem, whereas banana cultivation requires a large area, needs to be covered, and does not require penetration; hence, full cone is preferred.

Table 8: Field testing of flat fan nozzle.

Flow rate	UAV operating velocity	Area coverage for 10 litres	Time taken to cover 1 acre
2 litres/min		0.8 acre	7.05 min
3 litres/min	3 m/s	0.68 acre	7.05 min
4 litres/min		0.45 acre	7.05 min
2 litres/min		0.92 acre	5.56 min
3 litres/min	4 m/s	0.76 acre	5.56 min
4 litres/min		0.53 acre	5.56 min

Figure 29: Manual vs. UAV spraying.

(a) (b)

Figure 30: (a) UAV spraying. (b) Manual spraying.

Table 9: Type of crop and spray frequency.

Variety	Coimbatore 54
Crop type	Hybrid
Tillering stage	100 days to 120 days
No. of times sprayed	3 times (depending on the weather conditions and pest attack) After transplanting (i) First spray: tillering stage—28th day—pesticides (ii) Second spray: panicle initiation—50th day (iii) Third spray: pest's attack—62nd day

Table 10: Comparative study of manual spraying and UAV spraying.

Description	Manual spraying	UAV spraying
Crop	Paddy	Paddy
Area	1 acre	1 acre
Time taken to spray	2.5 hours	7 min
Crop damage	Yes	No
No. of people required	3	2
Water quantity required	100 litres	20 litres
Fertilizers/pesticides required	200 ml (depending on the type)	150 ml (usually 20% less than manual)
Operating cost	Rs 40 per tank. For 1 acre, manual spray 10 tanks = Rs 400 Labor cost for mixing the pesticides and water on an average = Rs 100 per acre Supply the meals to the operator = Rs 100 Total = Rs 600 per acre	Battery cost = Rs 100 per acre Operator cost = Rs 200 per acre Labor cost for mixing the pesticides and water on an average = Rs 100 per acre Total = Rs 400 per acre
Area coverage per day	Maximum of 3 acres per person	20 acres per UAV
Yield obtained	2.4 tons per acre	2.8 tons per acre

5. Conclusion and Future Work

The endurance of UAVs is dependent on the overall weight and usage of battery motors and propellers. As the trend for the usage of UAVs is increasing and the government of India's policy is favouring the usage of UAVs in farming, it is necessary to develop an affordable UAV with better endurance to make the small- and medium-scale farmers use this technology. As part of this research, it was aimed to reduce the weight of the UAV to increase the endurance of UAVs. The purpose is to minimize chemical use and maximize battery life by determining the optimal nozzle and operating parameters based on the link between pressure and the area covered. To effectively implement precision farming, it is necessary to develop an AI system to identify the crop stress level. Based on this research, the following conclusions are made:

(1) The reduction in weight of the body increased the UAV's endurance by 10% under no load conditions, and in the full load conditions, it was reduced by 8% as compared to commercially available UAVs

(2) The usage of materials for UAV is one of the important factors in deciding the overall weight of the UAV. The design changes are made in the arm structure, which reduced the weight by 5%. The weight reduction was achieved by selecting lightweight materials without compromising the factor of safety. Both arm sections were manufactured with ABS material. The larger section was attached to the fuselage, and the smaller section held the propeller. Both were screw jointed. The structural stability of the arm was analysed in FEA and found to be well within the limit and offered a factor of safety of 6

(3) The UAV component selection and the thrust measurement to lift a 10 kg payload were experimentally measured in a custom-made experimental setup for 3 propeller sizes. It was found that a 23-inch propeller was the most energy-efficient propeller for a given agricultural UAV

(4) With selected materials and custom-made arms, the weight was reduced by 5%, and the cost was reduced by 30%

(5) The relationship between nozzles for their orifice diameters vs. pressure and cone was established. The performance of nozzles was measured experimentally and found that the minimum pressure required is 4 bar to achieve a good cone angle and large coverage area. Suggestions on the selection of nozzle and operating conditions were given for 5 crops which are cultivated largely in Tamil Nadu, India

(6) To enable precision farming, the usage of AI is necessary; hence, in this work, a dataset of lemon leaf images was created. The processing of the images was analysed using CNN, random forest, and logistic regression techniques. It was found that the CNN was more suitable due to the 99% accuracy it yielded with nearly 30% less computational time as compared with the other two

After the detailed explanation of this work's conclusions, the possible extensive study from this work is also given below for further action:

(1) Although this work was limited to the change of material and structure of arms, it is necessary to try the combination of materials to reduce the weight. For instance, the larger part of the arm can still be ABS, and the smaller section could be made with carbon fibre. It will not reduce the weight and may increase the payload capacity

(2) Overall structural analysis by changing the materials of landing gear, frames, and tanks needs to be conducted to investigate the effect on overall weight

(3) Although this work is more focused on establishing the nozzle performance parameters, droplet size needs to be measured. Further, it can also be analysed for very high pressures

(4) The research concluded that CNN is the best suit for precision farming, it is necessary to implement it in the UAV and analyse the consumption of chemicals. Further, it is necessary to create the UAV dataset for stress levels for plants such as paddy, guava, turmeric, and areca nut which are widely cultivated in the state of Tamil Nadu, India

Abbreviations

ASABE: American Society of Agricultural and Biological Engineers
AI: Artificial intelligence
BLDC: Brushless direct current
CCCI: Canopy chlorophyll content index
C_L: Coefficient of lift
Kv: Constant velocity of a motor
ρ: Density of the atmospheric fluid
k: Design constant
D_f: Diameter of the fuselage
DGCA: Directorate General of Civil Aviation
A: Disc area of the propeller
D: Drag
η: Efficiency
ESC: Electronic speed controller
FEA: Finite element analysis
GPS: Global positioning system
GDP: Gross domestic product
L: Length of the fuselage
L_{UAV}: Length of the UAV
LiPo: Lithium polymer
P: Mechanical power required
NDVI: Normalized difference vegetation index
W_O: Overall take-off weight
W_{Pl}: Payload weight
PDPA: Phase Doppler Particle Analyzer
θ: Pitch angle
r: Radius of the propeller
λ: Taper ratio
T: Thrust
UAV: Unmanned aerial vehicles
UAS: Unmanned aircraft system
V_{UAV}: Velocity at forward maneuvering
V_o: Velocity of the atmospheric fluid
V_e: Velocity of the UAV
VTOL: Vertical take-off and landing.

Data Availability

The authors confirm that the data supporting the findings of this study are available within the article.

Conflicts of Interest

The authors declare no conflict of interest.

Authors' Contributions

Darshan Kumar Jayaram, Beena Stanislaus Arputharaj, and Vijayanandh Raja were responsible for the conceptualization. Darshan Kumar Jayaram, Vijayanandh Raja, Hussein A. Z. AL-bonsrulah were responsible for the methodology. Beena Stanislaus Arputharaj and Hussein A. Z. AL-bonsrulah were responsible for the validation. Darshan Kumar Jayaram and Vijayanandh Raja were responsible for the formal analysis. Vijayanandh Raja, Beena Stanislaus Arputharaj, and Hussein A. Z. AL-bonsrulah were responsible for the investigation. Darshan Kumar Jayaram was responsible for the resources. Darshan Kumar Jayaram and Vijayanandh Raja were responsible for the data curation. Darshan Kumar Jayaram and Vijayanandh Raja were responsible for the writing—original draft preparation. Beena Stanislaus Arputharaj and Hussein A. Z. AL-bonsrulah were responsible for the writing—review and editing. Beena Stanislaus Arputharaj and Hussein A. Z. AL-bonsrulah were responsible for the supervision. Darshan Kumar Jayaram, Vijayanandh Raja, Beena Stanislaus Arputharaj, and Hussein A. Z. AL-bonsrulah were responsible for the project administration. Vijayanandh Raja was responsible for the funding acquisition. All authors have read and agreed to the published version of the manuscript.

References

[1] P. Guhathakurta and M. Rajeevan, "Trends in the rainfall pattern over India," *Journal of Climatology*, vol. 28, no. 11, pp. 1453–1469, 2008.

[2] P. K. Maddikunta, S. Hakak, M. Alazab et al., "Unmanned aerial vehicles in smart agriculture: applications, requirements, and challenges," *IEEE Sensors Journal*, vol. 21, no. 16, pp. 17608–17619, 2021.

[3] S. Kumar, M. E. Answer, T. K. Immanuelraj et al., "Agricultural wages in India: trends and determinants," *Agricultural Economics Research Review*, vol. 33, no. 1, pp. 71–79, 2020.

[4] N. Peppes, "The role of drones as an enabler for the 4th agricultural revolution," *Current Research in Agricultural Sciences*, vol. 7, no. 2, pp. 40–51, 2020.

[5] K. Chiranjeeb and R. Beuria, "Role and application of UAVs for smart agriculture," *Biotica Research Today*, vol. 2, no. 8, pp. 702-703, 2020.

[6] F. De Rango, G. Potrino, M. Tropea, A. F. Santamaria, and N. Palmieri, "Simulation, modeling and technologies for UAVs coordination techniques in precision agriculture," in *International Conference on Simulation and Modeling Methodologies, Technologies and Applications*, pp. 77–101, Springer, Cham, 2019.

[7] M. J. Kumar, "The sky is not the limit: the new rules give wings to the drone technology in India," *IETE Technical Review*, vol. 38, no. 5, pp. 463-464, 2021.

[8] B. Drury, J. Valverde-Rebaza, M. F. Moura, and A. de Andrade Lopes, "A survey of the applications of Bayesian networks in agriculture," *Engineering Applications of Artificial Intelligence*, vol. 65, pp. 29–42, 2017.

[9] A. King, "Technology: the future of agriculture," *Nature*, vol. 544, no. 7651, pp. S21–S23, 2017.

[10] S. R. Juhi Reshma and A. S. Pillai, "Impact of machine learning and Internet of Things in agriculture: state of the art," in *International Conference on Soft Computing and Pattern Recognition*, pp. 602–613, Springer, 2016.

[11] J. Sihag and D. Prakash, "A review: importance of various modeling techniques in agriculture/crop production," in *Soft Computing: Theories and Applications. Advances in Intelligent Systems and Computing*, K. Ray, T. Sharma, S. Rawat, R. Saini, and A. Bandyopadhyay, Eds., vol. 742, Springer, Singapore, 2019.

[12] V. Gautam and S. Sarkar, "Smart agriculture: the age of UAVs in agriculture," in *International Conference on Unmanned Aerial System*, pp. 415–424, Geomatics Springer, Cham, 2020.

[13] A. L. K. A. Rani, A. M. R. E. S. H. Chaudhary, N. Sinha, M. Mohanty, and R. Chaudhary, "UAV: the green technology for future agriculture," *HaritDhara*, vol. 2, no. 1, pp. 3–6, 2019.

[14] P. Garre and A. Harish, "Autonomous agricultural pesticide spraying UAV," *Art*, vol. 455, 2018.

[15] H. Chen, H. Jin, B. Xu, and J. Xu, "A survey on security challenges in edge computing: attacks, defenses, and opportunities," *IEEE Transactions on Network Science and Engineering*, vol. 8, no. 1, pp. 62–77, 2021.

[16] P. Psirofonia, V. Samaritakis, P. Eliopoulos, and I. Potamitis, "Use of unmanned aerial vehicles for agricultural applications with emphasis on crop protection: three novel case-studies," *International Journal of Agricultural Science and Technology*, vol. 5, no. 1, pp. 30–39, 2017.

[17] H. Guler, H. Zhu, H. E. Ozkan, R. C. Derksen, Y. Yu, and C. R. Krause, "Spray characteristics and drift reduction potential with air induction and conventional flat-fan nozzles," *American Society of Agricultural and Biological Engineers*, vol. 50, no. 3, pp. 745–754, 2007.

[18] F. A. Vega, F. C. Ramírez, M. P. Saiz, and F. O. Rosúa, "Multitemporal imaging using an unmanned aerial vehicle for monitoring a sunflower crop," *Biosystems Engineering*, vol. 132, pp. 19–27, 2015.

[19] D. E. Martin, W. E. Woldt, and M. A. Latheef, "Effect of application height and ground speed on spray pattern and droplet spectra from remotely piloted aerial application systems," *Drones*, vol. 3, no. 4, p. 83, 2019.

[20] J. Liao, Y. Zang, X. Luo et al., "Optimization of variables for maximizing efficacy and efficiency in aerial spray application to cotton using unmanned aerial systems," *International Journal of Agricultural and Biological Engineering*, vol. 12, no. 2, pp. 10–17, 2019.

[21] H. Huang, J. Zhang, Y. Liu, and X. Sun, "UAV-based cooperative search and rescue using multi-objective optimization," *IEEE Access*, vol. 6, pp. 7504–7513, 2018.

[22] I. D. Pharne, S. Kanase, S. Patwegar, P. Patil, A. Pore, and Y. Kadam, "Agriculture drone sprayer," *International Journal of Recent Trends in Engineering & Research (IJRTER)*, vol. 4, no. 3, pp. 181–185, 2018.

[23] J. A. Gomes, N. M. Rodrigues, and F. J. Ferreira, "Unmanned aerial vehicles (UAVs) in the context of industry 5.0 in agriculture: a systematic literature review," *Sensors*, vol. 21, no. 7, p. 2467, 2021.

[24] D. Yallappa, M. Veerangouda, D. Maski, V. Palled, and M. Bheemanna, "Development and evaluation of drone mounted sprayer for pesticide applications to crops," in *2017*

IEEE Global Humanitarian Technology Conference (GHTC), pp. 1–7, San Jose, CA, USA, 2017.

[25] S. P. Yeong and S. S. Dol, "Aerodynamic optimization of micro aerial vehicle," *Journal of Applied Fluid Mechanics*, vol. 9, no. 7, pp. 2111–2121, 2016.

[26] V. Raja, S. K. Solaiappan, P. Rajendran, S. K. Madasamy, and S. Jung, "Conceptual design and multi-disciplinary computational investigations of multirotor unmanned aerial vehicle for environmental applications," *Applied Sciences*, vol. 11, no. 18, p. 8364, 2021.

[27] B. Y. Suprapto, M. A. Heryanto, H. Suprijono, J. Muliadi, and B. Kusumoputro, "Design and development of heavy-lift hexacopter for heavy payload," in *2017 International Seminar on Application for Technology of Information and Communication (iSemantic)*, pp. 242–247, Semarang, Indonesia, 2017.

[28] J. Kim, S. Kim, C. Ju, and H. I. Son, "Unmanned aerial vehicles in agriculture: a review of perspective of platform, control and applications," *IEEE Access*, vol. 7, pp. 105100–105115, 2019.

[29] M. F. F. Rahman, S. Fan, and Y. Z. L. Chen, "A comparative study on application of unmanned aerial vehicle systems in agriculture," *Agriculture*, vol. 11, no. 1, p. 22, 2021.

[30] K. Agrawal and P. Shrivastav, "Multi-rotors: a revolution in unmanned aerial vehicle," *International Journal of Science and Research (IJSR)*, vol. 4, no. 11, pp. 1800–1804, 2015.

[31] V. Puri, A. Nayyar, and L. Raja, "Agriculture drones: a modern breakthrough in precision agriculture," *Journal of Statistics and Management Systems*, vol. 20, no. 4, pp. 507–518, 2017.

[32] M. N. Sudin, F. R. Ramli, M. R. Alkahari, and M. A. Abdullah, "Comparison of wear behavior of ABS and ABS composite parts fabricated via fused deposition modelling," *International Journal of Advanced and Applied Sciences*, vol. 5, no. 1, pp. 164–169, 2018.

[33] A. Gong and D. Verstraete, "Experimental testing of electronics speed controllers for UAVs," in *53rd AIAA/SAE/ASEE Joint Propulsion Conference*, pp. 1–10, Atlanta, GA, 2017.

[34] A. K. verma, N. K. Pradhan, R. Nehra, and Prateek, "Challenge and advantage of materials in design and fabrication of composite UAV," *IOP Conference Series: Materials Science and Engineering*, vol. 455, no. 1, article 012005, 2018.

[35] K. Rahnamai, "Quadrotor UAVs thrust measurement apparatus," in *IEEE Aerospace Conference*, pp. 1–6, Big Sky, MT, USA, 2016.

[36] W. AJAnemaat, M. Schuurman, W. Liu, and A. Karwas, "Aerodynamic design, analysis and testing of propellers for small unmanned aerial vehicles," American Institute of Aeronautics and Astronautics, 2017.

[37] G. Andria, A. DiNisio, A. M. L. Lanzolla, G. Percoco, and G. Stano, "Design and characterization of innovative 3D printed embedded strain gauges," in *2019 IEEE 5th International Workshop on Metrology for AeroSpace (MetroAeroSpace)*, pp. 54–59, Turin, Italy, 2019.

[38] C. Koparan, A. B. Koc, C. V. Privette, and C. B. Sawyer, "Autonomous in situ measurements of noncontaminant water quality indicators and sample collection with a UAV," *Water*, vol. 11, no. 3, p. 604, 2019.

[39] C. E. Tinney and J. Sirohi, "Multirotor drone noise at static thrust," *AIAA Journal*, vol. 56, no. 7, pp. 2816–2826, 2018.

[40] M. Rizon, C. K. Ang, M. I. Solihin et al., "Effects of variable arm length on UAV control systems," *Journal of Robotics, Networking and Artificial Life*, vol. 7, no. 2, pp. 91–97, 2020.

[41] J. L. Carranza-Flores, M. Martínez-Arroyo, J. A. Montero-Valverde, and J. L. Hernández-Hernández, "Search for damage of the citrus miner to the lemon leaf, implementing artificial vision techniques," in *Technologies and Innovation. CITI 2020. Communications in Computer and Information Science*, R. Valencia-García, G. Alcaraz-Marmol, J. Cioppo-Morstadt, N. Vera-Lucio, and M. Bucaram-Leverone, Eds., vol. 1309, Springer, Cham, 2020.

[42] K. Kiratiratanapruk, P. Temniranrat, A. Kitvimonrat, W. Sinthupinyo, and S. Patarapuwadol, "Using deep learning techniques to detect rice diseases from images of rice fields," in *Artificial Intelligence Theory and Applications*, vol. 12144 of Lecture Notes in Computer Science, Springer, Cham, 2020.

[43] J. Darshan Kumar, R. Thottungal, and R. Vijayanandh, "Effective monitoring by drone using advanced deep machine learning strategies with IoT," *Journal of Environmental Protection and Ecology*, vol. 22, no. 3, pp. 1246–1258, 2021.

[44] U. R. Mogili and B. B. V. L. Deepak, "Review on application of drone systems in precision agriculture," *Procedia Computer Science*, vol. 133, pp. 502–509, 2018.

[45] G. Balaganesh, G. Makarabbi, S. Niranjan, and S. Ashokkumar, "Agricultural land utilization in India," *Indian Farmer*, vol. 4, no. 8, pp. 596–599, 2017.

[46] T. O. Mogorosi, R. S. Jamisola, N. Subaschandar, and L. O. Mohutsiwa, "Thrust-to-weight ratio optimization for multirotor drones using neural network with six input parameters," in *2021 International Conference on Unmanned Aircraft Systems (ICUAS)*, pp. 1194–1199, Athens, Greece, 2021.